Water Research 291 (2026) 125248

Contents lists available at ScienceDirect

Water Research

journal homepage: www.elsevier.com/locate/watres

Revealing the optimal ratio of aged-to-fresh carbon in BAC filtration: linking biofilm development, iDNA/eDNA community dynamics, and purification performance

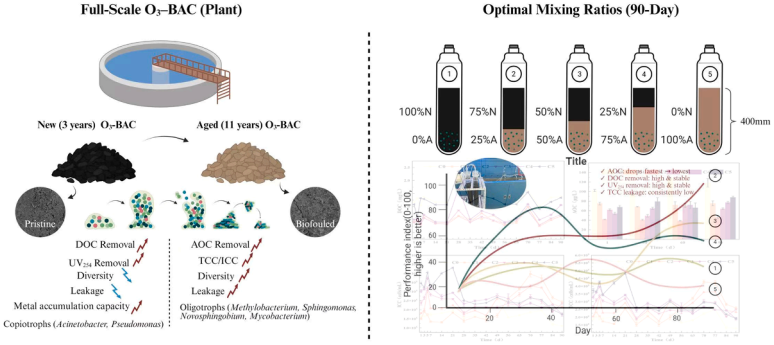
Yu Zhou [a], Xin Song [a], Weiying Li [a,c,*], Xiaojing Luo [b], Chengrui Yang [b]

[a] College of Environmental Science and Engineering, Tongji University, Shanghai, 200092, PR China
[b] College of River and Ocean, Chongqing Jiaotong University, Chongqing 400074, PR China
[c] Key Laboratory of Yangtze River Water Environment, Ministry of Education, Tongji University, 1239 Siping Road, Shanghai, 200092, PR China

HIGHLIGHTS

- Full-scale and lab-scale studies reveal optimal BAC replacement strategies.
- Intermediate ratios balance adsorption capacity and biofilm biodegradation.
- iDNA/eDNA analysis decodes microbial succession and ecological resilience.
- Biofilm diversity and stability determine long-term pollutant removal.
- Findings guide carbon renewal practices for safe and stable water treatment.

GRAPHICAL ABSTRACT



ARTICLE INFO

Keywords:
O_3-BAC;Carbon replacement ratio;Biofilm;
Microbial community dynamics;Drinking water

ABSTRACT

Ozone-biological activated carbon (O_3-BAC) filtration has been widely employed for water purification, yet guidance on appropriate strategies for carbon media renewal remains unclear. A pair of full-scale O_3-BAC filters located at a water treatment plant in eastern China (new: 3 years; aged: 11 years) was investigated and verified with a 90-day lab-scale test comprising four columns spanning 0–100% fresh carbon to decipher adsorption-biodegradation interactions and microbial succession. In the full-scale system, the newer filter removed 21.99% of dissolved organic carbon (DOC) and reduced UV_{254} by 20.14%, whereas the aged filter, despite its weaker adsorption, removed more assimilable organic carbon (AOC, 22.67%) consistent with a mature biofilm but released more cells to the effluent (up to 2.2×10^5 mL^{-1}). In the laboratory, beds filled only with fresh carbon showed strong early adsorption but slower onset of nitrification and a delayed decline in AOC, while beds filled only with aged carbon provided immediate biodegradation but higher start-up cell release. Critically, intermediate replacement synchronized adsorption and biodegradation: the 75% fresh + 25% aged configuration stabilized fastest, drove residual AOC towards about 20 μg L^{-1} by day 90, and maintained effluent cell concentrations on the order of 10^3–10^4 mL^{-1} while developing dense, diverse biofilms. Microbial analysis showed that hybrid beds preserved nitrifiers and aromatic degraders from aged media while recruiting pioneer colonizers

* Corresponding author.
E-mail address: 123lwyktz@tongji.edu.cn (W. Li).

https://doi.org/10.1016/j.watres.2025.125248
Received 22 October 2025; Received in revised form 29 November 2025; Accepted 19 December 2025
Available online 25 December 2025
0043-1354/© 2025 Elsevier Ltd. All rights are reserved, including those for text and data mining, AI training, and similar technologies.

on fresh carbon, enabling broad-spectrum removal of protein-like and humic-like organics confirmed by three-dimensional fluorescence spectroscopy. These findings indicate that partial rather than full replacement, optimally 50–75% fresh carbon, can maximize organic pollutant removal and minimize microbial risks when BAC operation maintains low and stable AOC, low and steady effluent TCC/ICC, and concurrent declines in UV_{254} and DOC, providing a practical basis for sustainable BAC management under stringent drinking water standards.

1. Introduction

Urban drinking water sources in China face substantial contamination, posing significant challenges for compliance with the recently updated National Standards for Drinking Water Quality (GB5749–2022). These stringent regulations necessitate enhancements in water treatment technologies, with ozone-biological activated carbon (O_3-BAC) filtration emerging as a preferred method due to its effectiveness in removing refractory organic pollutants and improving biological stability(Blair et al., 2024; Zhang et al., 2025). The combined ozonation and activated carbon processes significantly enhance organic pollutant biodegradability, enabling biofilm-mediated degradation on carbon surfaces, yet potential risks such as microbial leakage and activated carbon exhaustion threaten water safety (Fu et al., 2017; Hamid et al., 2019; Peng et al., 2025; Teel et al., 2022; Terry and Summers, 2018). Consequently, it is crucial to thoroughly understand microbial community dynamics and contaminant removal efficiency, particularly during the operational transition from fresh to aged activated carbon.

Previous studies and global applications have consistently highlighted the efficacy of O_3-BAC in reducing dissolved organic carbon (DOC), ammonia nitrogen, color, and disinfection by-product precursors across water treatment plants in Germany, Australia, Japan, and China (Kato et al., 2018; Liu et al., 2024). However, performance varies significantly depending on activated carbon properties, biofilm characteristics, operational parameters (e.g., ozone dose, empty bed contact time, and backwashing strategy), and the competitive adsorption between natural organic matter (NOM) and micropollutants (Blachnio et al., 2025; Quan et al., 2023; Ray and Roy, 2013; Selmi et al., 2024; Yang et al., 2010). Biofilm formation, governed by extracellular polymeric substances (EPS), substantially impacts contaminant biodegradation efficiency and system stability, thus serving as a key monitoring parameter for evaluating biological activated carbon (BAC) operational performance (Fundneider et al., 2021; Gibert et al., 2013; Kirchen et al., 2024; Rosenqvist et al., 2025; Salama et al., 2016; Zhou et al., 2021). Despite reduced adsorption capacity, aged activated carbon supports adapted microbial communities beneficial for biodegradation when mixed with fresh carbon, underscoring the importance of optimal carbon replacement strategies to balance performance and safety (Chen et al., 2020; Tao et al., 2020).

This study aims to systematically evaluate the optimal ratio of aged-to-fresh activated carbon by comparing organic pollutant removal efficiency, microbial community structure, and biofilm characteristics using advanced analytical methods such as high-throughput 16S rRNA sequencing, three-dimensional fluorescence excitation-emission matrix (3D-EEM) spectroscopy, and intra- and extracellular DNA analysis. By elucidating these interactions at both full-scale and laboratory scales, the research will provide critical theoretical foundations and practical guidelines for activated carbon management in drinking water treatment plants. Ultimately, the findings will enhance microbial safety, optimize carbon replacement practices, and ensure compliance with stringent water quality standards, thereby addressing both operational and public health concerns in drinking water production.

2. Materials and methods

2.1. Sampling sites and experimental setup

2.1.1. Full-Scale experiments at the water treatment plant

In this study, both new and aged BAC samples were collected from a full-scale water treatment plant located in a city in eastern China. The new BAC filter was commissioned in 2021 and had been in operation for 3 years at the time of sampling, whereas the aged BAC filter was commissioned in 2013 and had been operating for 11 years. At this plant, only two full-scale O_3-BAC filters are available; the 3-year unit was selected as the youngest bed beyond the start-up phase, while the 11-year unit represents a late-service “aged” bed with reduced adsorption but a well-developed biofilm. (Shi et al., 2024; Song et al., 2021). Both filters utilized coal-based granular activated carbon, and key design and operating parameters of the full-scale O_3-BAC filters are summarized in Table S1. The plant draws raw water from a major river in a southeastern Chinese city, with the treatment process comprising pre-ozonation, high-density clarification, upflow plate filtration, O_3-BAC filtration, and chlorine disinfection, as illustrated in Figure. S1. During coagulation, polyaluminum chloride and polyacrylamide were added. Ozone was dosed at 0.4–1.0 mg/L, ensuring that residual ozone at the outlet of the contactor was zero to prevent any potential impact on downstream filtration units.

Water samples (50 L each) from the influent and effluent of both new and aged O_3-BAC filters, as well as BAC media samples (1 kg each), were collected in sterile containers. BAC samples were taken from the upper layer of each filter bed, stored in sterile bags, and maintained at 4 °C during transportation to the laboratory for subsequent analysis. Detailed raw water quality parameters for the plant are provided in Table S2.

To investigate the differences in organic matter removal and microbial community dynamics between new and aged O_3-BAC filters, sampling was performed every 30 days over three stages, designated as Stage 1, Stage 2, and Stage 3. The influent to the O_3-BAC filter was denoted as INF, the effluent of the new filter as NEFF, and that of the aged filter as OEFF. Biofilm samples from the new and aged BAC were labeled as NBAC and OBAC, respectively. Details of microbial sample codes are provided in Table S3.

To evaluate the effects of backwashing on organic removal and microbial community composition, samples were also collected from the new and aged O_3-BAC filters before and after backwashing. The plant employed an air-water backwashing regimen with an 8-day interval. Sampling was conducted over three cycles (Cycle 1, Cycle 2, Cycle 3). The new filter before and after backwashing were denoted as XQ and XH, respectively, while the aged filter before and after backwashing were denoted as JQ and JH. Corresponding biofilm samples were labeled as XQM (new filter, pre-backwash), XHM (new filter, post-backwash), JQM (aged filter, pre-backwash), and JHM (aged filter, post-backwash). Details of the microbial sample codes for these samples are summarized in Table S4. A schematic overview of the full-scale O_3-BAC system, including all water and biofilm sampling locations, is provided in Figure S2.

2.1.2. Laboratory-Scale experiments for optimizing carbon replacement ratios

Laboratory-scale experiments were conducted using five custom-designed acrylic column reactors (outer diameter: 80 mm; height: 600 mm; wall thickness: 5 mm; bottom outlet: 3 mm; threaded inlet cap: 3

mm). The new carbon used in these tests was virgin coal-based granular activated carbon, while the aged carbon was sourced from the aforementioned plant and had been in service for 11 years.

Five groups with different new-to-aged BAC ratios were established and packed in the reactors as follows:

C1: 100 % new carbon (bed height: 400 mm);

C2: 75 % new + 25 % aged carbon (bed heights: 300 mm and 100 mm, respectively);

C3: 50 % new + 50 % aged carbon (both 200 mm);

C4: 25 % new + 75 % aged carbon (100 mm and 300 mm, respectively);

C5: 100 % aged carbon (bed height: 400 mm).

All columns operated in down-flow mode. In C2-C4, new and aged BAC were arranged as stratified layers, with new carbon on the influent side overlying aged media, simulating full-scale practice in which only the upper portion of the bed is renewed while deeper aged media is retained. The bottom of each reactor was layered with quartz sand (bed height: 50 mm; particle size: 0.55–1.2 mm) as a supporting layer. The influent for all reactors was post-sand filter effluent from the full-scale plant, delivered via a six-channel peristaltic pump at a flow rate of 15 mL/min, resulting in an empty bed contact time of 30 min. An additional group, denoted as C0, was set up as the influent control, representing the raw influent water sample prior to BAC filtration. The experiment was operated continuously for 90 days, during which water quality and biomass of effluent, BAC, and biofilm samples from each group were monitored. The configuration of the laboratory BAC columns (C0-C5) and their new/aged carbon mixing ratios is illustrated in Figure S2. The experimental setup is illustrated in Figure. S3, and the codes for BAC biofilm microbial samples are detailed in Table S5.

2.2. Water quality and BAC performance analysis

Temperature measurements for the influent and effluent of the O_3-BAC filters were performed on-site. Water samples from both influent and effluent were subsequently transported to the laboratory for comprehensive analysis, including pH, turbidity, UV_{254} absorbance, DOC, heavy metal ions, anions, total cell counts (TCC), and intact cell counts (ICC). For biofilm analysis, ~50 g wet BAC was suspended in 100 mL ultrapure water in sterile 250 mL flasks, vortexed for 30 s, and subjected to low-energy bath sonication (60 W, 40 kHz, 5 min) to detach cells. A 5 min sonication time was selected from optimisation tests (2–10 min) that maximised total and intact cell counts, while longer durations reduced cell recovery and viability. (Text S1, Table S6 and Figure S4) (Vignola et al., 2018; Wan et al., 2019). Prior to analysis, both water and biofilm suspensions were filtered through a 0.45 μm membrane to remove suspended solids and insoluble organic matter. Detailed analytical methods and parameters for each water quality indicator are summarized in Table S7.

2.3. The 3D-EEM spectroscopy

The 3D-EEM spectroscopy was conducted using a fluorescence spectrophotometer (Hitachi F-4500, Japan). Excitation wavelengths ranged from 200 to 500 nm, and emission wavelengths ranged from 200 to 550 nm, both with increments of 2 nm. The scanning speed was set at 30,000 nm/min. Water samples were filtered through a 0.45 μm membrane, and a 3 mL aliquot was placed into a 1 cm quartz cuvette for analysis. Milli-Q ultrapure water (Millipore, resistivity 18.25 MΩ·cm) served as the blank control. Raman scattering was corrected by subtracting the blank ultrapure water spectra, and Rayleigh scattering interference was eliminated by zeroing the spectral data above the Rayleigh scattering region.The EEM fluorescence spectra were partitioned into five discrete regions, with each region representing a particular class of organic compounds (Wells et al., 2022). Comprehensive details regarding this classification are provided in Table S8.

2.4. Biomass and assimilable organic carbon (AOC) analysis

Biomass was quantified using flow cytometry to measure TCC and ICC, providing a rapid, accurate, and convenient alternative to traditional heterotrophic plate counting (HPC). Detailed procedures for AOC determination, including P17/NOX cultivation, flow-cytometric calibration, and method-performance parameters (regression equations, R^2, LOD/LOQ and precision), are provided in Text S2, Figure S13 and Table S12 (Li et al., 2022, 2019; Zhang et al., 2019).

2.5. Intracellular DNA (iDNA) and extracellular DNA (eDNA) extraction

Water samples from the O_3-BAC system were filtered through a 0.22 μm polyethersulfone (PES) membrane and a nucleic acid adsorption particle (NAAP) column to collect iDNA and eDNA, respectively (Gu et al., 2024). The filtration setup was shown in Figure S5. iDNA and eDNA were then extracted and purified using commercial kits following the manufacturers' protocols. Biofilm samples from BAC media were processed similarly after detachment of attached biomass. iDNA and eDNA concentrations were quantified using a Qubit fluorometer. Detailed procedures are provided in Text S3.

2.6. 16S rRNA high-throughput sequencing

Genomic DNA was extracted from both water and activated-carbon biofilm samples using the PowerWater® DNA Isolation Kit (MoBio, USA) according to the manufacturer's instructions, yielding 50 μL per sample that was stored at −80 °C. The bacterial community structure was interrogated by Illumina paired-end (2 × 250 bp) sequencing of the V3-V4 hypervariable region of the 16S rRNA gene, amplified with primers 338F (ACTCCTACGGGAGGCAGCA) and 806R (GGACTACHVGGGTWTCTAAT)(Attiani et al., 2025; Cholet et al., 2025; Perrin et al., 2019). Each 50 μL PCR comprised 25 μL Taq polymerase, 2 μL of each primer (10 μM), 1 μL bovine serum albumin, 50 ng template DNA and nuclease-free water. Thermocycling was 95 °C for 2 min; 30 cycles of 95 °C for 20 s, 53 °C for 20 s, 72 °C for 20 s; and a final 72 °C extension for 5 min. Amplicons were confirmed on 1 % agarose gels, quantified with GeneTools (v4.03.05.0), pooled in equimolar amounts, purified with the E.Z.N.A.® Gel Extraction Kit (Omega, USA) and eluted in TE buffer. Libraries were prepared with the ALFA-SEQ DNA Library Prep Kit, their fragment sizes assessed on a Qsep400 analyzer and concentrations determined with a Qubit 4.0 fluorometer (Thermo Fisher Scientific, USA) prior to sequencing.

The raw 16S rRNA gene sequencing data are deposited in the NCBI Sequence Read Archive (SRA) under BioProject PRJNA706168 (run accession SRR13838637; https://www.ncbi.nlm.nih.gov/bioproject/PRJNA706168)

2.7. Physicochemical characterization of fresh and aged BAC

Characterization encompassed N_2 adsorption-desorption (BET, t-plot, BJH, NLDFT) for specific surface area and pore architecture, powder XRD (d_{002}, Lc), ATR-FTIR for functional groups, FE-SEM for morphology, and EDS for elemental composition and mapping. Fresh and aged BAC were analyzed under identical protocols. Full procedures, instrument configurations, and quality controls are provided in Text S4.

2.8. Statistical analysis

Statistical analyses were performed in R (version 4.1) and OriginPro 2025. Data were checked for normality and homogeneity of variance. Differences between new and aged filters were tested with paired or independent *t*-tests. One-way ANOVA with Tukey's post-hoc test was used to compare treatments (C0-C5).

3. Results and discussion

3.1. Full-scale performance: organic/inorganic pollutant removal in aged vs. new BAC filters

The full-scale evaluation compared the performance of new and aged O_3-BAC filters in removing organic and inorganic contaminants, with a focus on DOC, UV_{254} absorbance, and selected metal ions (Fig. 1). INF DOC averaged 1.89 ± 0.58 mg/L, characteristic of riverine drinking-water sources in eastern China and indicative of a low-to-moderate organic load (Li et al., 2023). Effluent concentrations from the NEFF and OEFF were 1.45 ± 0.32 mg/L and 1.60 ± 0.31 mg/L, corresponding to mean removal efficiencies of 21.99 ± 6.80 % and 13.17 ± 11.34 %, respectively. The superior DOC removal by the new filter likely reflects its higher adsorption capacity and greater efficacy in eliminating disinfection by-product (DBP) precursors. Similar trends were observed

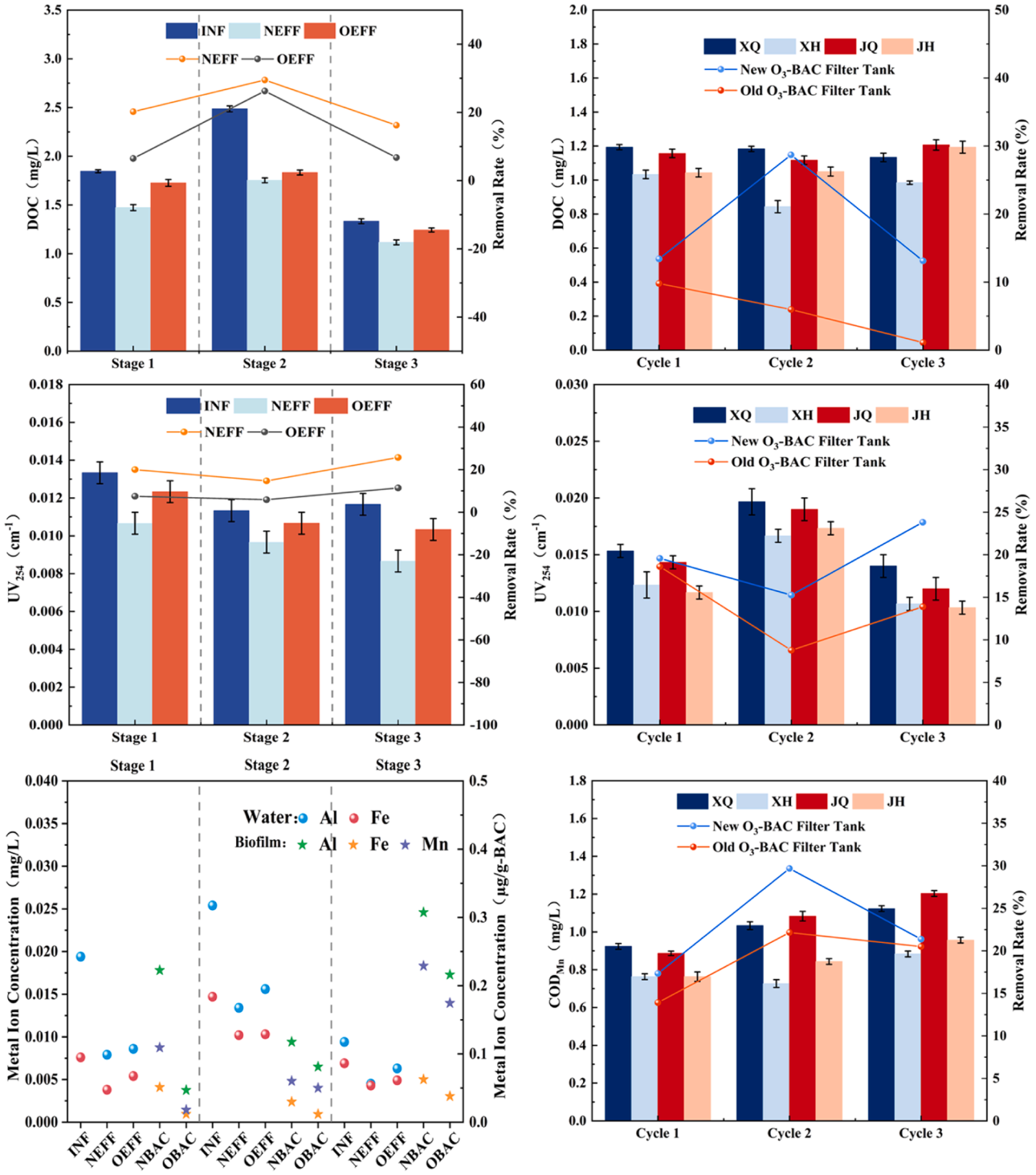


Fig. 1. Performance of new and aged O_3-BAC filters in removing organic and inorganic pollutants. (A) DOC in INF, NEFF, and OEFF. (B) DOC before and after backwashing in XQ/XH and JQ/JH. (C) UV_{254} in INF, NEFF, and OEFF. (D) UV_{254} before and after backwashing in XQ/XH and JQ/JH. (E) Al, Fe, Mn in INF, NEFF, OEFF, NBAC, and OBAC. (F) COD_{Mn} before and after backwashing in XQ/XH and JQ/JH.

for UV_{254}, an indicator of aromatic organics: the new filter achieved a removal rate of 20.14 ± 5.51 %, compared with 8.27 ± 2.85 % for the aged filter ($p < 0.05$). These results indicate that filter aging markedly diminishes the adsorption of both bulk and aromatic organic matter, presumably due to carbon surface degradation and pore blockage over time.

For inorganic pollutants, aluminum (Al), iron (Fe), and manganese (Mn) concentrations in biofilms were consistently higher in NBAC than in OBAC. For instance, Al in the NBAC biofilm averaged 0.2159 ± 0.0951 μg/g, nearly double the 0.1147 ± 0.0894 μg/g measured in OBAC ($p < 0.05$). This suggests that newer carbon, with a less occluded surface and a more active biofilm, provides greater capacity for metal ion sequestration. In contrast, concentrations of major anions (Cl^-, SO_4^{2-}, NO_3^-) were largely unaffected by BAC filtration, consistent with their limited adsorption onto activated carbon surfaces (Figure S6). The backwashing influenced performance in both filters but to differing extents. Following backwashing, DOC removal averaged 18.41 % for the new filter and only 5.62 % for the aged filter, and this difference was statistically significant ($p < 0.05$), indicating a greater recovery of adsorption sites in the former. Similar patterns were observed for UV_{254} and COD_{Mn}, with the new filter exhibiting mean post-backwash removal rates of 19.54 % and 22.79 %, compared with 13.76 % and 18.85 % in the aged filter, respectively. These findings highlight that although routine backwashing can partially restore performance, it cannot offset the long-term decline associated with carbon aging. Consequently, timely carbon renewal is critical for sustaining the removal of organic matter and metal ions in full-scale BAC applications.

The fluorescence characteristics of DOM in influent and effluents of new and aged O_3-BAC filters were further examined using 3D-EEM spectroscopy (Fig. 2). Distinct differences in fluorescence intensity were observed, particularly in regions I, IV, and V, corresponding to protein-like substances, microbial metabolites, and humic substances, respectively. In the new filter, NEFF showed marked reductions in regions IV and V relative to INF ($p < 0.05$), indicating effective removal of humic-like and microbial-derived DOM. Fluorescence regional integration (FRI) analysis (Table 1) revealed removal efficiencies of 16.28 % (region II), 21.59 % (region III), and 20.96 % (region V) for NEFF.In contrast, OEFF exhibited increased fluorescence intensities in regions II, III, IV, and V, with negative removal efficiencies of −5.56 %, −29.07 %, and −18.68 % in regions I, II, and V, respectively (Table 1). These results suggest that the aged filter not only failed to remove certain DOM fractions but also leached protein-like and humic-like compounds into the effluent.

Backwashing had differing impacts on the two filters. For the new filter, XH showed slight improvements over XQ in the removal of protein-like substances (regions I and II) and microbial metabolites (region III), with removal efficiencies of 5.90 %, 1.39 %, and 4.76 %, respectively (Table 1). However, humic substance removal (region V) decreased (Δ6.21 %), suggesting limited restoration of adsorption capacity for these higher-molecular-weight, more recalcitrant compounds. Corresponding water quality parameters (Table S9) indicated that backwashing reduced turbidity (e.g., 0.22 to 0.137 NTU in Cycle 1) and increased dissolved DO from 6.99 to 8.07 mg/L, supporting partial recovery of biofilm activity.In the aged filter, JH exhibited negligible improvement compared with JQ; removal efficiencies remained negative for most regions, with values of −4.03 % in region II and −5.56 % in region III, with only a marginal gain for humic substances (Δ6.26 %) (Table 1). Water quality changes (Table S9) were minimal, with turbidity decreasing slightly (e.g., 0.159 to 0.123 NTU in Cycle 1) and DO increasing modestly (from 8.07 to 8.25 mg/L), consistent with

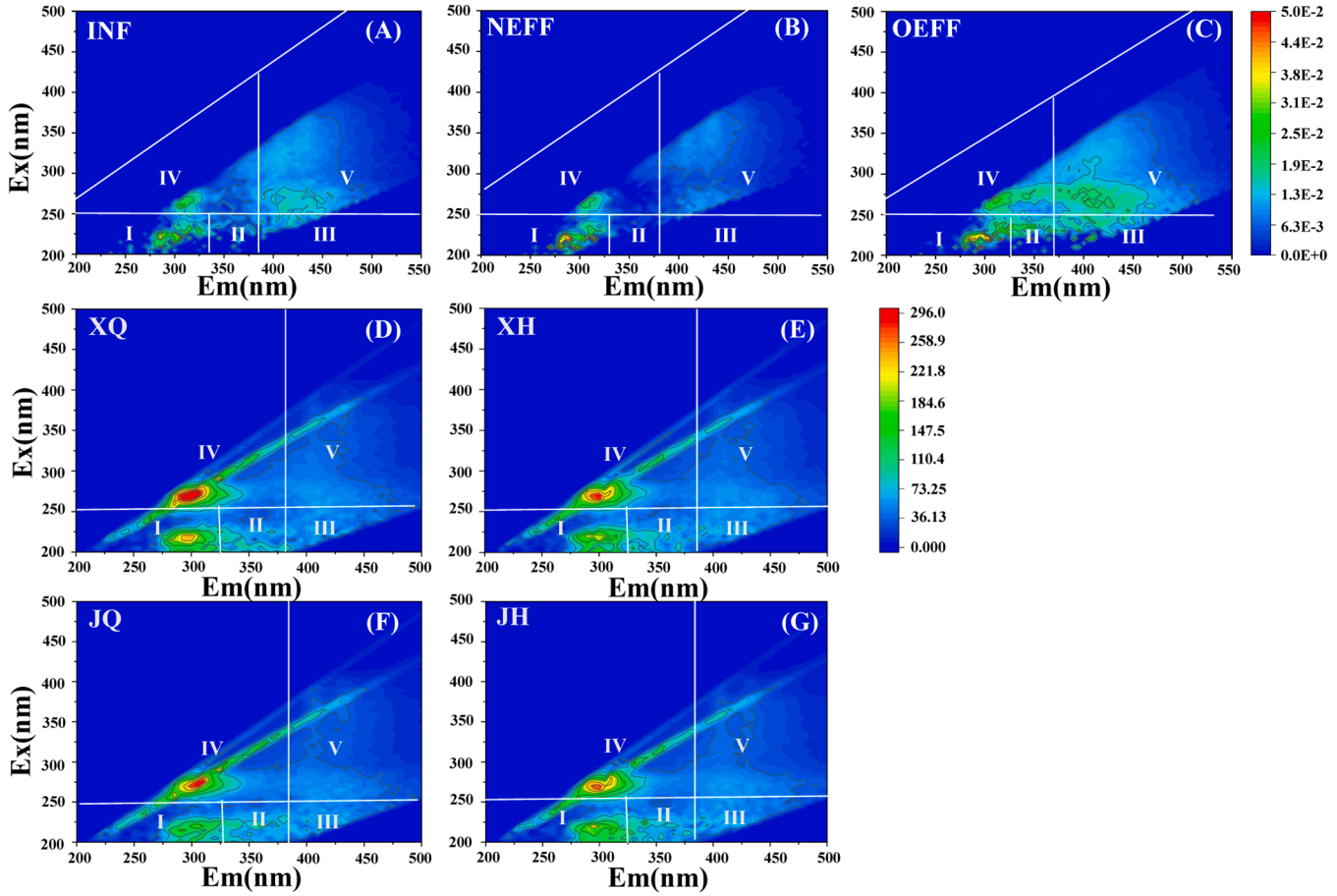


Fig. 2. EEM fluorescence spectra of DOM in new and aged O_3-BAC filters. (A-C) INF, NEFF, and OEFF. (D-G) XQ/XH and JQ/JH before and after backwashing.

Table 1
Integrated FRI results of DOM before and after O_3-BAC filtration and backwashing in new and aged filters. ΦT, n denotes the normalized volume in each region, and RE (%) indicates the relative change compared to previous stage.

Sample ID	Region I		Region II		Region III		Region IV		Region V	
	ΦT, n	RE (%)	ΦT, n	RE (%)	ΦT, n	RE (%)	ΦT, n	RE (%)	ΦT, n	RE (%)
INF	0.198	–	0.086	–	0.088	–	0.466	–	0.439	–
NEFF	0.200	−1.01	0.072	16.28	0.069	21.59	0.434	6.87	0.347	20.96
OEFF	0.209	−5.56	0.111	−29.07	0.103	−17.05	0.515	−10.52	0.521	−18.68
XQ	0.356	–	0.144	–	0.147	–	0.934	–	0.725	–
XH	0.335	5.90	0.142	1.39	0.140	4.76	0.903	3.32	0.770	−6.21
JQ	0.335	–	0.149	–	0.144	–	0.878	–	0.733	–
JH	0.322	3.88	0.155	−4.03	0.152	−5.56	0.823	6.26	0.734	−0.14

Note: Negative RE (%) values indicate release or increase in fluorescence intensity.

limited biological and adsorptive regeneration. These results indicate that the new O_3-BAC filter (NEFF/XH) retained the ability to remove a broad spectrum of DOM components and that backwashing partially restored its performance. In contrast, the aged filter (OEFF/JH) exhibited substantial functional decline, with persistent release of protein-like and humic-like substances, underscoring the importance of timely carbon replacement to sustain long-term filtration efficiency.

Complementary material characterizations corroborate the full-scale trends. Figure S7 and Table S10 show clear surface/structural aging of BAC: XRD/FTIR indicate increased surface oxidation (e.g., Si-O-Si/O—H features) and loss of aromatic/alkyl signals in aged media, while SEM (200 nm and 10 μm) reveals smoother, infilled surfaces with micro-cracking relative to the rougher, more open texture of new BAC. Figure S8 and Table S11 further demonstrate lower N_2 uptake and a redistribution/partial loss of small mesopores in aged BAC from BJH analysis, consistent with pore blocking and reduced effective surface area. Together, these changes explain why the new filter exhibits stronger adsorption of bulk and aromatic NOM (higher DOC and UV_{254} removal), lower effluent cells, and greater metal accumulation in biofilm, whereas the aged filter shows weakened adsorption but enhanced biodegradation capacity (higher AOC removal) accompanied by greater biomass leakage. These converging lines of evidence reinforce that routine backwashing cannot reverse material aging; sustaining full-scale performance requires timely carbon renewal and optimized replacement ratios.

3.2. Microbial risks in full-scale systems: from biomass accumulation to biofilm leakage

Microbial risks in full-scale O_3-BAC filtration systems were assessed by examining AOC, microbial biomass in water (TCC, ICC), and biofilm-associated biomass, as well as the effects of backwashing across three operational cycles (Fig. 3). AOC concentrations in INF, NEFF, and OEFF averaged 86.87 ± 31.06, 75.59 ± 24.69, and 67.88 ± 27.13 μg/L, respectively. Both filters effectively reduced AOC to levels below the 100 μg/L threshold for biological stability. Interestingly, the aged filter achieved higher average AOC removal (22.67 ± 4.05 %) than the new filter (12.35 ± 4.87 %) ($p < 0.05$), suggesting that biofilm maturity in OBAC may enhance biodegradation. Before backwashing, AOC in XQ was 129.67 ± 1.79 μg/L, higher than in JQ (98.41 ± 7.21 μg/L) ($p < 0.05$). After backwashing, AOC decreased to 55.68 ± 10.33 μg/L in XH and 31.25 ± 25.21 μg/L in JH, indicating that while the new filter showed a greater absolute reduction, the aged filter maintained stronger biodegradative capability (Fig. 3B).

TCC and ICC were consistently higher in OEFF compared with INF and NEFF, particularly in Stage 2. For example, TCC averaged $1.5 \times 10^5 \pm 5.2 \times 10^4$ cells/mL in INF, $1.8 \times 10^5 \pm 6.1 \times 10^4$ in NEFF, and $2.2 \times 10^5 \pm 8.0 \times 10^4$ in OEFF, while ICC reached $7.1 \times 10^4 \pm 3.4 \times 10^4$, $9.7 \times 10^4 \pm 4.0 \times 10^4$, and $1.3 \times 10^5 \pm 4.0 \times 10^4$ cells/mL, respectively (Fig. 3C, E), and intact cell release (ICC) in OEFF was significantly higher than in NEFF ($p < 0.05$). This indicates that both filters released microbial cells, but aged BAC was more prone to leakage. Backwashing reduced microbial loads in both systems, yet JQ/JH consistently exhibited higher TCC and ICC than XQ/XH, with the aged filter releasing approximately 24,907 ± 14,381 cells/mL after backwashing compared with only 7167 ± 883 cells/mL for the new filter (Fig. 3D, F). Consistent with this, post-backwashing decreases in ICC and TCC were significantly greater in the aged than in the new filter (both $p < 0.05$). This suggests stronger biofilm detachment in aged filters due to more developed microbial communities.Fig. 4.

Biofilm biomass confirmed this trend, as OBAC consistently showed higher TCC and ICC than NBAC across all stages. In Stage 1, OBAC contained $6.9 \times 10^6 \pm 2.5 \times 10^6$ (TCC) and $4.2 \times 10^6 \pm 1.6 \times 10^6$ cells/g (ICC), compared to $5.2 \times 10^6 \pm 3.1 \times 10^6$ and $3.0 \times 10^6 \pm 1.7 \times 10^6$ cells/g in NBAC. This divergence increased in Stage 2, where OBAC values were nearly double those in NBAC, and biofilm ICC and TCC in OBAC were significantly higher than in NBAC ($p < 0.05$). After backwashing, both systems showed reductions, but OBAC decreased more substantially (195,182 ± 37,485 cells/g vs. 92,385 ± 31,663 cells/g in NBAC), and this greater decrease in biofilm TCC was statistically significant ($p < 0.05$), indicating that aged biofilms harbored greater biomass but were more prone to detachment during hydraulic disturbance.

Overall, both filters effectively reduced AOC, but microbial accumulation and detachment were substantially greater in aged filters (OEFF, JQ/JH, OBAC). The elevated ICC in OBAC underscores the persistence of viable cells, which contributes to microbial leakage and poses risks to biological stability in treated water. Regular monitoring and timely carbon replacement are therefore essential to mitigate microbial risks and sustain long-term biological safety in full-scale O_3-BAC operations.

3.3. Microbial community succession: decoding the black box of BAC functionality

The microbial community dynamics within new and aged O_3-BAC filters reveal critical insights into biological activated carbon functionality, reflecting substantial shifts in microbial diversity, structure, and ecological roles. Analysis of eDNA and iDNA across INF, NEFF and OEFF, and corresponding biofilms (NBAC, OBAC) captured marked differences in richness and diversity, strongly associated with filter age and operational stage. Intracellular DNA typically displayed higher microbial richness than eDNA in water samples, suggesting an active microbial community distinct from extracellular remnants. Conversely, eDNA richness dominated biofilm matrices, indicating significant accumulation of extracellular DNA over operational periods due to cell turnover and biofilm maturation. As shown in Figure S9, α- and β-diversity analyses based on iDNA and eDNA, including ACE and Chao1 richness estimators, Shannon and Simpson indices, rarefaction curves, and PCoA of Bray-Curtis distances, reveal clear clustering by filter age and treatment stage (INF/NEFF/OEFF; NBAC/OBAC). Consistent with our interpretation, iDNA from water samples generally exhibits greater richness, whereas eDNA accumulation within biofilms, particularly in OBAC, is more pronounced, corroborating the succession from copiotrophic to

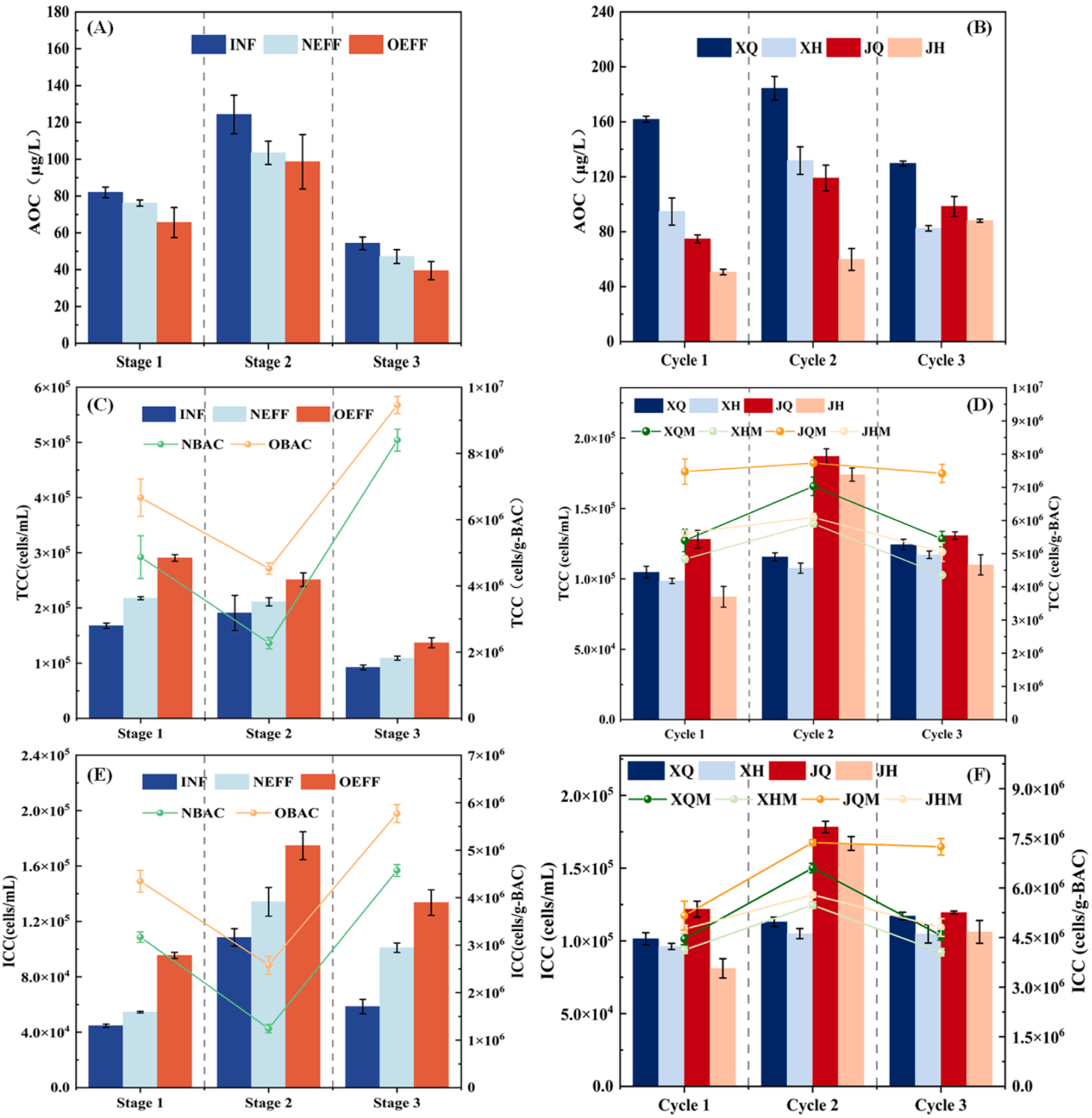


Fig. 3. Dynamics of AOC, TCC, and ICC in new and aged O_3-BAC filters. (A) AOC in INF, NEFF, and OEFF across stages. (B) AOC in XQ/XH and JQ/JH before and after backwashing over three cycles. (C) TCC in water and biofilm (NBAC, OBAC) from INF, NEFF, and OEFF. (D) TCC in water and biofilm for XQ/XH, JQ/JH (water) and XQM/XHM, JQM/JHM (biofilm) before and after backwashing. (E) ICC in water and biofilm from INF, NEFF, OEFF, NBAC, and OBAC. (F) ICC in water and biofilm for XQ/XH, JQ/JH (water) and XQM/XHM, JQM/JHM (biofilm) before and after backwashing.

oligotrophic assemblages.

Initial colonization of the NBAC was characterized by copiotrophic taxa, predominantly Acinetobacter and Pseudomonas, thriving on easily biodegradable organic compounds. These genera initially dominated both biofilm and effluent phases but declined markedly with prolonged operation. Successional shifts were pronounced, transitioning from dominance by opportunistic heterotrophs towards more specialized, oligotrophic taxa in the OBAC. Notably, genera such as *Methylobacterium-Methylorubrum, Sphingomonas, Novosphingobium*, and *Mycobacterium* as well as canonical nitrifiers such as *Nitrospira* and *Nitrosomonas* progressively increased their relative abundance, reflecting adaptation to more refractory organic substrates and complex ecological niches. *Sphingomonas* and *Novosphingobium* are well documented degraders of mono- and polyaromatic compounds and other recalcitrant NOM fractions, while *Mycobacterium* and related *Actinobacteria* can attack hydrophobic organic matter; *Nitrospira* and *Nitrosomonas* form the key nitrite- and ammonia-oxidizing guilds responsible for biological nitrification in drinking water biofilters (Zhao et al., 2022).The rise of these taxa aligns with an enhanced capacity for biodegradation of recalcitrant organic matter and transformation of the DBP precursors, critical for water quality stabilization and biological safety.

Comparative community analysis between biofilms and effluents revealed the pivotal role of BAC biofilms as both microbial sinks and sources. The aged filter effluent exhibited higher microbial diversity and richness ($p < 0.05$), closely resembling its biofilm community,

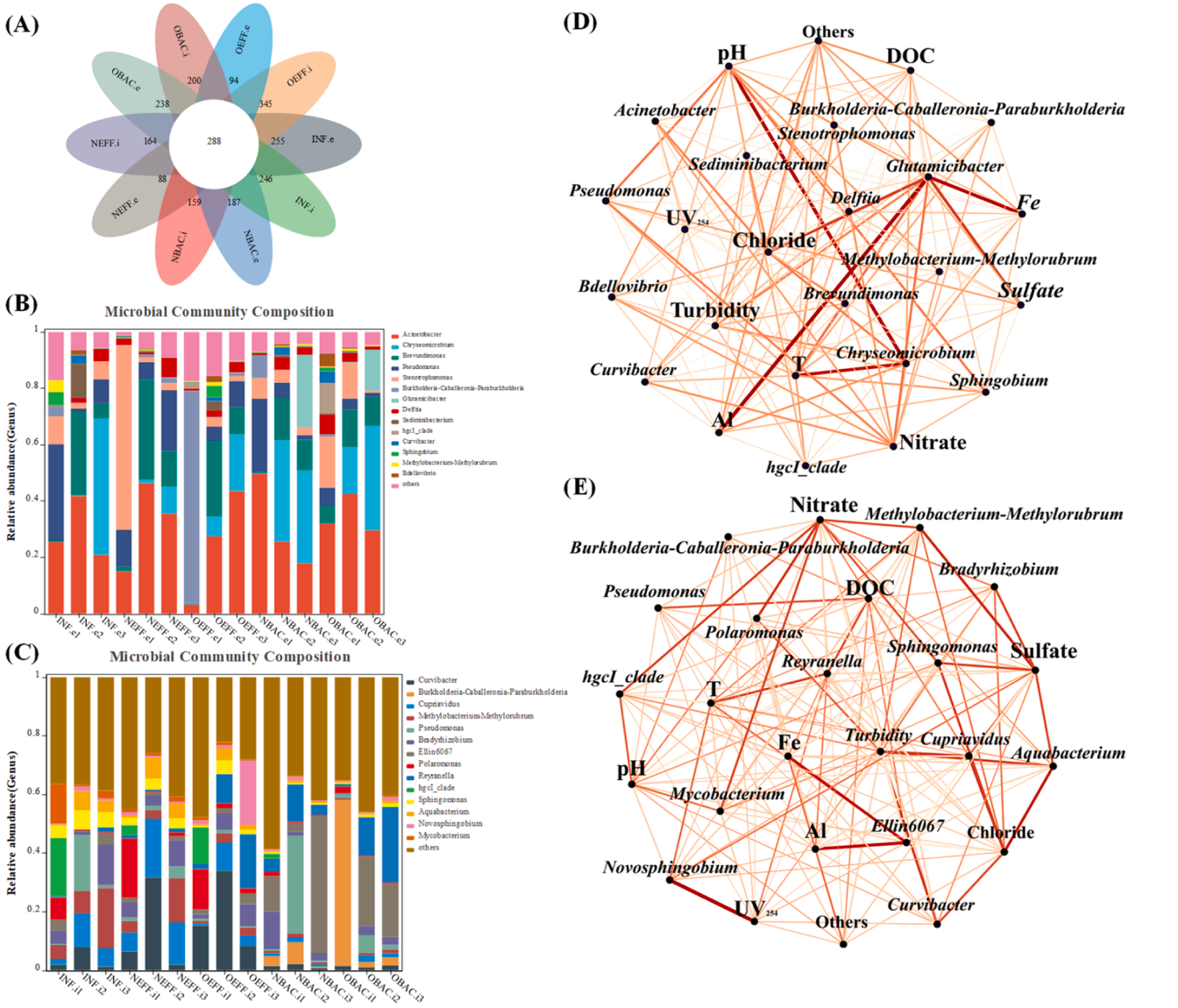


Fig. 4. Microbial community composition and co-occurrence networks in extracellular and intracellular fractions. (A) Venn diagram of shared and unique OTUs among samples.(B) Genus-level community composition in the extracellular fraction.(C) Genus-level community composition in the intracellular fraction.(D) Co-occurrence network of extracellular microbial communities and environmental factors.(E) Co-occurrence network of intracellular microbial communities and environmental factors.

indicating consistent microbial sloughing into treated water. In particular, iDNA based profiles of OEFF increasingly mirrored those of OBAC, whereas eDNA retained a stronger imprint of historical biofilm communities. Biofilms maintained distinct compositions, enriched in surface-associated and slow-growing bacteria, while effluent communities often included more planktonic or loosely attached microbes. Consequently, the effluent microbial profile evolved significantly from influent water, highlighting biofilm communities' substantial influence on microbial water quality. The enrichment of *Nitrospira* and *Nitrosomonas* in OBAC iDNA suggests that nitrifying biofilm clusters are an important source of nitrifier export to the aged-filter effluent, consistent with the sustained nitrate production observed in Stage 2 (Fujitani et al., 2020).

Network co-occurrence analyses illuminated critical microbial interactions with water quality parameters such as DOC, UV_{254} absorbance, and inorganic ions. Genera such as *Novosphingobium* and *Sphingomonas*, known for aromatic compound degradation, positively correlated with UV_{254} and DOC, signifying their pivotal role in NOM transformation. Similarly, *Methylobacterium* demonstrated associations with nitrate and sulfate, implicating its involvement in nutrient cycling within the biofilm ecosystem. Nitrifying taxa (mainly *Nitrospira* and *Nitrosomonas*) showed positive associations with nitrate and dissolved oxygen, supporting their assignment to the nitrifying functional guild, and linking nitrification activity to aged BAC biofilms (Zhao et al., 2022). Metal ions like aluminum and iron correlated strongly with taxa such as *Acinetobacter* and *Chryseobacterium*, suggesting their potential roles in metal-associated particle formation or transformation processes. Increased network complexity observed in aged filters indicated enhanced ecological interconnectedness and niche specialization, crucial for efficient pollutant degradation and system resilience.

The consistent presence of these microbes in aged filter effluent underscores an important trade-off: while a mature microbial community enhances NOM removal and DBP precursor degradation, it simultaneously increases microbial biomass release and potential pathogen presence. Thus, strategically timed carbon replacement or media regeneration becomes critical, effectively resetting microbial succession to mitigate health risks without compromising treatment efficiency. Alternatively, operational measures such as optimized backwashing,

targeted disinfection, or hybrid ozone-BAC systems can control biofilm biomass, balancing ecological benefits with microbial safety. This integrated microbial-ecological perspective emphasizes leveraging biofilter maturity to maximize water purification potential while proactively managing biofilm dynamics to ensure biologically safe and stable drinking water quality in long-term BAC operations.

Across three operational cycles, distinct differences in microbial community metrics were evident between new (X) and aged (J) O_3-BAC filters, both before (Q) and after (H) backwashing. The aged BAC biofilms consistently exhibited higher microbial richness and diversity than the new filters. For instance, the aged filter's Shannon diversity index remained substantially higher than that of the new filter even immediately after backwashing (JH vs. XH), indicating that the more developed biofilm was less affected by backwashing. As shown in Figure S10, Alpha

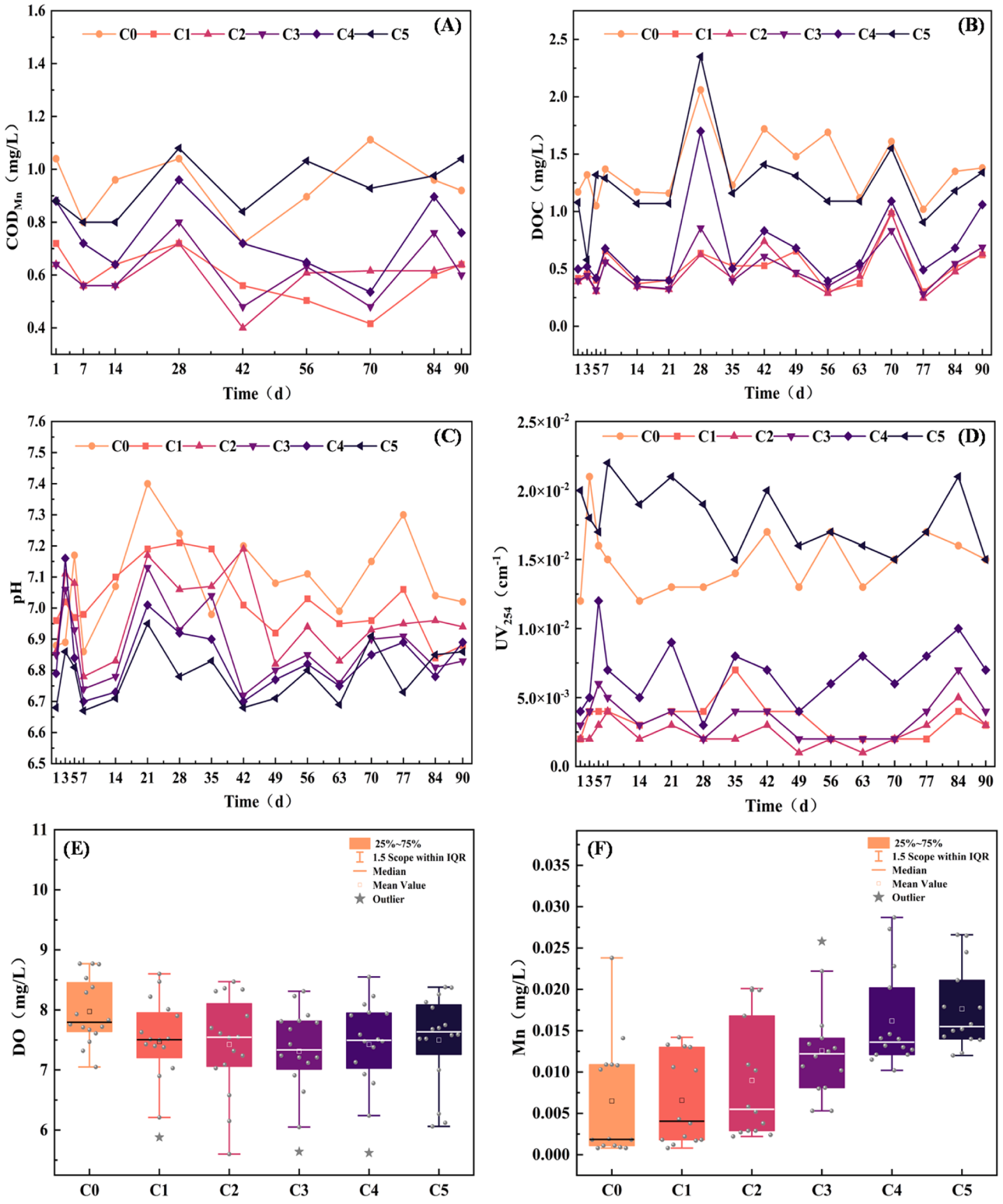


Fig. 5. Variations of (A) COD_{Mn}, (B) DOC concentrations, (C) pH, (D) UV_{254}, (E) dissolved oxygen (DO), and (F) Mn ion concentrations over a 90-day operation period under different mixing ratios of new and aged BAC.

diversity measures such as ACE were also greater and more persistent in the aged filter, with only minor reductions post-backwash compared to the more pronounced drops observed in the new filter. These results demonstrate a stronger resistance to backwashing in aged communities. Taxonomic profiling further highlighted the resilience of the aged filter's microbiota. *Proteobacteria* was the dominant phylum in all samples, but the aged filter supported a broader array of taxa (e.g., additional *Bacteroidetes/Sphingobacteria* and others), contributing to its higher richness. Notably, community composition in the aged filter changed little with backwashing the relative abundances of key taxa before vs. after wash remained similar, suggesting a stable core biofilm. In contrast, the new filter's community structure shifted more noticeably after backwashing, reflecting the disruption of a less mature biofilm. Even when backwashing removed a substantial portion of biomass (up to approximately 50 % of attached cells), the aged biofilm rapidly regained its original diversity and abundance within days. Backwashing significantly reduced certain less adherent groups (e.g., *Sphingobacteria*) in deeper filter layers, yet the overall OTU count and Shannon index in the aged filter returned to near pre-backwash levels, accompanied by a relative increase in resilient taxa like *Proteobacteria*. These findings indicate that routine backwashing fails to fully disrupt the established microbial communities in aged BAC filters. This biofilm resilience has important implications for full-scale operation and carbon replacement strategies. The higher and persistent diversity observed in aged filters means that biological degradation capacity remains robust over extended filter life, but it also means standard backwashing is insufficient to reset the biofilm. Plant operators should therefore optimize backwashing intervals, as overly frequent backwashing of aged filters may waste water and energy without significantly reducing microbial biomass (given the rapid regeneration). Instead, backwashing schedules can be aligned with hydraulic performance needs, while relying on carbon replacement to manage long-term biofilm accumulation. Indeed, a point will be reached when even post-backwash microbial indices remain high, signaling that the biofilm has reached a resilient steady state. At that threshold, replacing or regenerating the BAC media is advisable to prevent excessive biofilm buildup and potential water quality concerns (e.g., elevated effluent bacteria). These results suggest that to optimize O_3-BAC filter performance and longevity, operators should extend carbon service life until biofilm growth approaches a stable maximum, implement backwashing at practical intervals for headloss control, and plan carbon renewal once microbial resilience indicates that routine backwashing no longer yields incremental benefits in biomass control.

3.4. Lab-scale optimization: determining the optimal carbon replacement ratio

3.4.1. Effects of BAC replacement ratio on water quality and pollutant removal

During the 90-day operation, filters with different mixing ratios of new and aged BAC (C0-C5) exhibited distinct trends in water quality improvement and biofilm development. As shown in Fig. 5A-D, increasing the proportion of new BAC enhanced the initial removal of COD_{Mn}, DOC, and UV_{254}, whereas aged BAC provided immediate biodegradation through its pre-established biofilm. Columns with higher proportions of new BAC (C3-C5) achieved faster and greater reductions in COD_{Mn} and DOC compared with aged-dominant systems (C0-C1). For example, C5 (100 % new BAC) exhibited the most pronounced early decreases in COD_{Mn} and UV_{254}, while C0 (100 % aged BAC) showed slower but steady declines dominated by biological oxidation. Among the intermediate ratios, C2 sustained the broadest and most consistent reductions across all organic parameters (Fig. 5A, B, D), reflecting the synergistic contribution of adsorption from new BAC and biodegradation from aged BAC.

Effluent pH remained stable (7.2–7.5) across all treatments (Fig. 5C) indicating negligible acid-base shifts. Dissolved oxygen dynamics (Fig. 5E) highlighted differences in microbial activity. C0 and C1 showed lower DO from the beginning, consistent with active respiration in aged BAC biofilms, whereas C4 and C5 maintained higher DO initially due to limited microbial consumption. Over time, DO decreased across all systems as biofilms matured, and by day 90 the values converged. Nitrate production followed a similar trajectory: C0 and C1 displayed higher concentrations at the outset, while C4 and C5 showed delayed increases, eventually approaching comparable levels (Figure S11E). These findings suggest a transient lag in nitrification in new-BAC-rich systems, which resolved once nitrifying communities established.Inorganic parameters revealed transient startup effects. Columns containing higher proportions of new BAC (C4-C5) showed brief increases in trace metals such as Cu, Zn, and Fe (Figures S11A-C), attributable to leaching from fresh media, but concentrations returned to baseline within several days. Chloride and sulfate remained stable regardless of BAC ratio (Figures S11D, F). Turbidity rose temporarily in C3-C5 due to carbon fines and biofilm disturbance, but effluent turbidity rapidly declined to below 1 NTU (Figure S11G), meeting drinking water clarity standards.

Fluorescence spectroscopy further clarified removal mechanisms. The 3D-EEM spectra (Figure S12) and FRI analysis (Table 1) demonstrated significant reductions in both protein-like (Regions I-II) and humic-like (Regions III-V) substances across all treatments. C5 achieved strong early removal of humic-like organics through adsorption, while C0 effectively degraded protein-like compounds due to mature biofilms but showed limited humic removal. Notably, C2 exhibited the greatest and most consistent reductions across all fluorescence regions, which showed significantly higher FRI removal in regions I-V than other columns at day 90 ($p < 0.05$), confirming that intermediate replacement ratios best integrate adsorption and biodegradation. The results highlight distinct performance patterns across the replacement spectrum: C0 and C1 relied mainly on biodegradation, C4 and C5 on adsorption with delayed microbial adaptation, while C2 provided the most balanced and sustained removal. These findings suggest that intermediate replacement ratios are optimal for stabilizing system performance, minimizing startup perturbations, and ensuring efficient long-term removal of diverse organic pollutants.

3.4.2. Impacts of BAC replacement ratio on biofilm development and microbial community structure

During the 90-day experiment, the six BAC columns (C0-C5) effectively disentangled the contributions of fresh adsorption (new BAC) and established biodegradation (aged BAC) and showed how their relative balance shapes microbial ecology and, in turn, system performance. Organic carbon dynamics provided the clearest evidence. COD_{Mn}, DOC, and UV_{254} declined in all treatments (Fig. 5A, B, D), but their trajectories diverged depending on the replacement ratio. Columns dominated by new BAC (C4, C5) exhibited steep early decreases, reflecting strong virgin adsorption, but removal leveled off as adsorption sites were progressively saturated and biofilms were still developing. In contrast, columns with more aged BAC (C0, C1) improved more gradually, driven primarily by microbial oxidation, but sustained removal through later stages. Intermediate mixtures (C2, C3) combined these mechanisms: they achieved rapid initial declines while maintaining steady long-term removal, ultimately outperforming both extremes. By day 90, C2 and C3 showed the most balanced and persistent reductions, illustrating that adsorption-biodegradation synergy was maximized at moderate replacement ratios.

AOC and DO trends further clarified the ecological underpinnings. Columns containing more aged BAC (C0, C1) rapidly lowered AOC concentrations while consuming oxygen from the start (Figs. 5E, 6A), a hallmark of pre-existing microbial activity. In contrast, all-new systems (C4, C5) retained high AOC and elevated DO initially, indicating limited microbial uptake, until biofilms matured and respiration increased. Nitrate accumulation patterns (Figure S11E) paralleled this divergence: C0 and C1 produced nitrate immediately, reflecting an established nitrifying community, whereas C4 and C5 lagged but eventually converged as nitrifiers colonized. The intermediate configurations (C2,

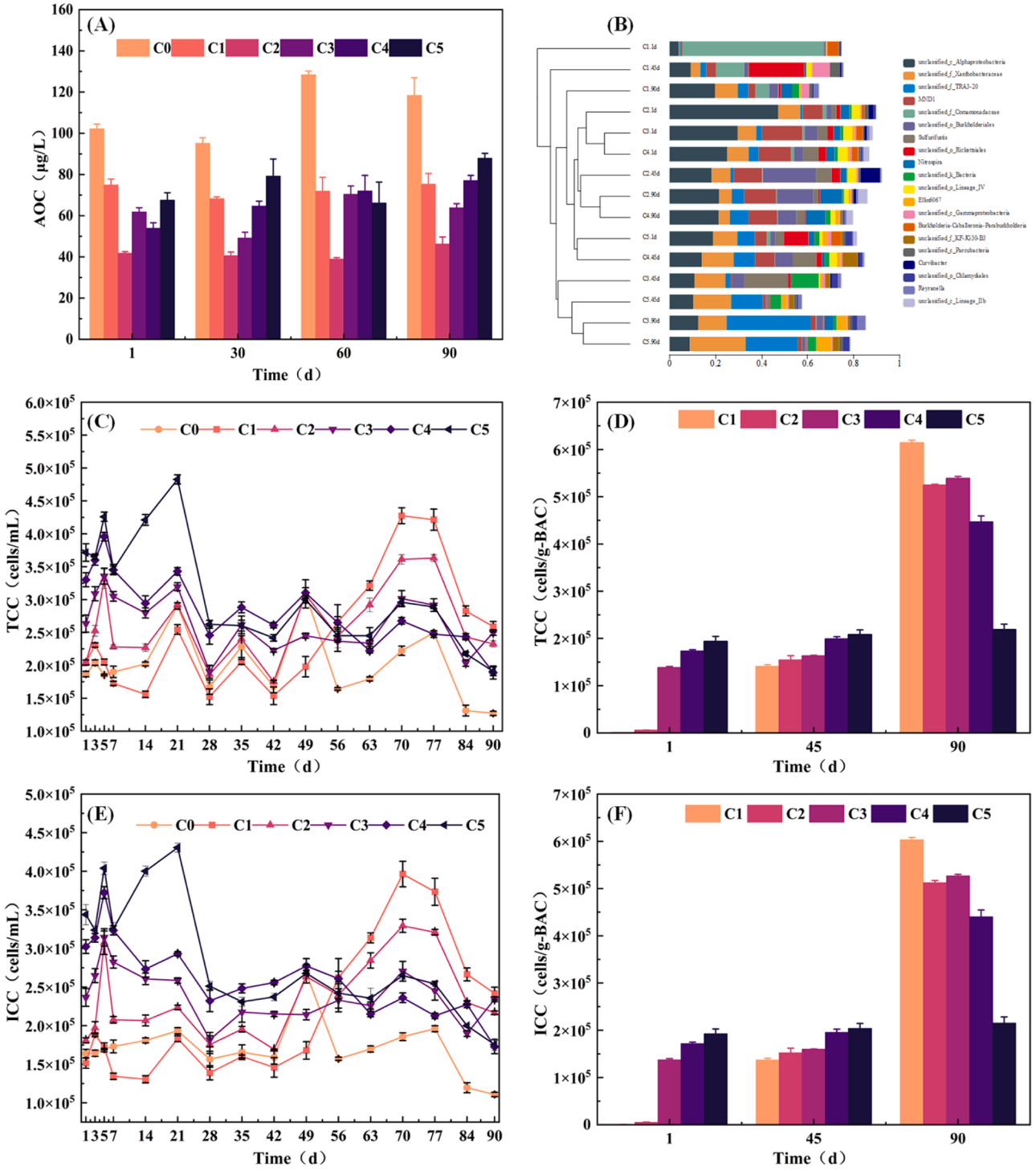


Fig. 6. Dynamics of AOC concentrations, microbial community composition at the genus level in biofilms, and microbial biomass represented by TCC and ICC in water and biofilm samples during a 90-day operational period for BAC columns with varying ratios of new and aged activated carbon. (A) AOC concentrations; (B) genus-level microbial community structure and clustering analysis of biofilms; (C) TCC in water samples; (D) TCC in biofilms; (E) ICC in water samples; (F) ICC in biofilms.

C3) avoided both extremes, showing smooth AOC declines and steady nitrate production, underscoring their ecological balance.

Cell counts in effluents illustrated the trade-off between biological stability and microbial leakage. Effluent TCC and ICC from C0 spiked sharply on day 1 due to sloughing of existing biomass, while those from C5 were near zero (Figs. 6C, E). Over time, all systems stabilized to low levels on the order of 10^3–10^4 cells/mL, but the path differed: C0 carried a short-term leakage risk, C5 required prolonged acclimation, and C2-C3 showed the lowest and most stable effluent counts throughout, highlighting their advantage for biological safety. Biofilm development within the media reinforced this conclusion. Columns with only aged BAC began with high attached biomass, while those with only new BAC started nearly sterile but accumulated exponentially (Figs. 6D, F). C2 and C3 showed the most favorable growth trajectory, rapidly building dense, viable biofilms seeded by aged BAC while exploiting the fresh surface area of new BAC. By day 90, their biofilm cell densities exceeded

those of the single-source systems, with significantly higher biofilm TCC/ICC ($p < 0.05$), consistent with their superior organic carbon removal. Sequencing data (Fig. 6B) revealed that these intermediate mixtures supported the most diverse and functionally versatile communities, combining legacy taxa from aged BAC (e.g., nitrifiers, aromatic degraders) with pioneer heterotrophs colonizing new surfaces. This hybrid structure enabled broad-spectrum degradation of both protein-like and humic-like organics, as confirmed by fluorescence spectroscopy (Figure S12, Table 1). By contrast, C0 remained dominated by a narrower, inherited community, while C5 was initially less diverse and slower to incorporate specialized degraders.

Inorganic parameters and operational stability echoed these trends. C4 and C5 experienced minor startup perturbations, including metal leaching and elevated turbidity (Figures S11A-C, G), while C0 and C1 showed higher oxygen demand and transient cell leakage. C2 and C3, by comparison, maintained smoother profiles for DO, NO_3^-, and turbidity, reflecting both faster stabilization and lower operational risk. pH remained stable across all treatments (Fig. 5C), and chloride and sulfate concentrations were unaffected (Figures S11D, F), indicating that replacement ratio primarily influenced biological, not chemical, pathways. These results tell a consistent story: new BAC provides strong but transient adsorption, aged BAC offers immediate but leakage-prone biodegradation, and only mixed strategies synchronize these processes in time and space. By coupling adsorption and microbial metabolism, C2 and C3 delivered the fastest stabilization, the most comprehensive organic removal, and the healthiest biofilm communities with minimal side effects. Practically, this means that moderate replacement ratios of 50–75 % new BAC combined with 25–50 % aged BAC are optimal. They minimize startup risks, maximize long-term efficiency, and sustain robust microbial diversity. In full-scale operation, this translates into three guidelines: (i) adopt partial replacement rather than full media change, ideally in the C2-C3 range; (ii) monitor AOC, DO, NO_3^-, and effluent cell counts to confirm synchronized adsorption-biodegradation; and (iii) treat high new-BAC replacements with caution, using seeding or staged startup to avoid delays in biological stabilization. By leveraging microbial ecology rather than working against it, operators can regenerate BAC filters more efficiently, extend media life, and ensure stable, biologically safe drinking water production.

4. Conclusions

In this study, full-scale monitoring of parallel O_3-BAC filters was combined with 90-day laboratory columns and multi-modal analyses to elucidate how the fresh-to-aged carbon ratio governs BAC performance. The main findings are:

- New versus aged BAC. New BAC achieved rapid, adsorption-driven removal of bulk and aromatic organics but required time to establish mature biofilms. In contrast, aged BAC exhibited diminished adsorption capacity but enhanced biodegradation and nitrification, accompanied by greater effluent cell release, indicating a trade-off between sorption capacity and biofilm maturity.
- Backwashing versus media ageing. Routine backwashing improved DOC and UV254 removal but did not restore long-term adsorption capacity or consistently mitigate biomass leakage, particularly in aged filters. Backwashing is therefore essential for hydraulic control but cannot substitute for media renewal.
- Synergy at mixed fresh-to-aged ratios. Columns packed solely with new BAC were dominated by adsorption with delayed biological stabilisation, whereas fully aged beds provided immediate biodegradation but higher start-up cell release. Intermediate replacement ratios of approximately 50–75 % fresh BAC mixed with 25–50 % aged BAC synchronised adsorption and biodegradation, yielded low residual AOC and stable effluent TCC/ICC, and supported diverse, well-developed biofilms capable of attenuating both protein-like and humic-like DOM.
- Operational implications. The results support partial, rather than complete, carbon replacement as the primary regeneration strategy. Thoroughly mixing 50–75 % fresh with 25–50 % aged BAC can shorten acclimation, enhance broad-spectrum NOM removal, and reduce microbial risks. Routine monitoring of AOC, DO, NO3−, effluent TCC/ICC and DOM fluorescence indices can be used to verify synchronised adsorption-biodegradation and to trigger media renewal when performance is no longer recoverable by backwashing alone.

Overall, this integrated full-scale and laboratory investigation provides a mechanistic and operational framework demonstrating that carefully managed partial carbon replacement can sustain high, stable and microbiologically safe BAC performance under increasingly stringent drinking-water standards.

Funding

This work was supported by the National Natural Science Foundation of China (Grant No. 52470012), the National Key R&D Program of China (Grant No. 2024YFC3810901–03), and the Fuzhou High-Quality Drinking Water Engineering Technical Consulting Service Project (Contract No. kh0040020211986).

CRediT authorship contribution statement

Yu Zhou: Writing – review & editing, Writing – original draft, Software, Methodology, Investigation, Data curation. **Xin Song:** Writing – review & editing, Methodology, Investigation. **Weiying Li:** Writing – review & editing, Project administration, Funding acquisition. **Xiaojing Luo:** Software, Methodology, Data curation. **Chengrui Yang:** Data curation.

Declaration of competing interest

The authors declare that they have no known competing financial interests or personal relationships that could have appeared to influence the work reported in this paper.

Supplementary materials

Supplementary material associated with this article can be found, in the online version, at doi:10.1016/j.watres.2025.125248.

Data availability

Data will be made available on request.

References

Attiani, V., Smidt, H., van der Wielen, P.W.J.J., 2025. Investigating spatial and temporal dynamics in microbial community composition of multiple full-scale slow sand filters in drinking water treatment. Water Res. 282.

Blachnio, M., Zienkiewicz-Strzalka, M., Derylo-Marczewska, A., 2025. Equilibrium adsorption of organic compounds (nitrobenzene derivative, synthetic pesticide, dye, and surfactant) on activated carbon from single- and multi-component systems. Molecules 30 (1).

Blair, M.F., Vaidya, R., Salazar-Benites, G., Bott, C.B., Pruden, A., 2024. Relating microbial community composition to treatment performance in an ozone-biologically active carbon filtration potable reuse treatment train. Water Res. 262.

Chen, S., Liu, C., Shen, H., Zhuang, X., Chen, W., 2020. Discussion on replacement strategy of invalidated biological activated carbon in drinking water plants. China Water Wastewater 36 (17), 49–56.

Cholet, F., Vignola, M., Quinn, D., Ijaz, U.Z., Sloan, W.T., Smith, C.J., 2025. Microbial ecology of drinking water biofiltration based on 16S rRNA sequencing: a meta-analysis. Water Res. 281.

Fu, J., Lee, W.N., Coleman, C., Nowack, K., Carter, J., Huang, C.H., 2017. Removal of disinfection byproduct (DBP) precursors in water by two-stage biofiltration treatment. Water Res. 123, 224–235.

Fujitani, H., Momiuchi, K., Ishii, K., Nomachi, M., Kikuchi, S., Ushiki, N., Sekiguchi, Y., Tsuneda, S., 2020. Genomic and physiological characteristics of a novel nitrite-

oxidizing nitrospira strain isolated from a drinking water treatment plant. Front. Microbiol. 11.
Fundneider, T., Alonso, V.A., Wick, A., Albrecht, D., Lackner, S., 2021. Implications of biological activated carbon filters for micropollutant removal in wastewater treatment. Water Res. 189.
Gibert, O., Lefèvre, B., Fernández, M., Bernat, X., Paraira, M., Calderer, M., Martínez-Lladó, X., 2013. Characterising biofilm development on granular activated carbon used for drinking water production. Water Res. 47 (3), 1101–1110.
Gu, J.-Y., Li, W.-Y., Zhou, Y., Zhang, G.-S., 2024. Environmental pollution and extraction methods of extracellular antibiotic resistance genes in water. Huan jing ke xue= Huanjing kexue 45 (12), 7041–7048.
Hamid, K.I., Sanciolo, P., Gray, S., Duke, M., Muthukumaran, S., 2019. Comparison of the effects of ozone, biological activated carbon (BAC) filtration and combined ozone-BAC pre-treatments on the microfiltration of secondary effluent. Sep. Purif. Technol. 215, 308–316.
Kato, R., Asami, T., Utagawa, E., Furumai, H., Katayama, H., 2018. Pepper mild mottle virus as a process indicator at drinking water treatment plants employing coagulation-sedimentation, rapid sand filtration, ozonation, and biological activated carbon treatments in Japan. Water Res. 132, 61–70.
Kirchen, F., Fundneider, T., Gimmel, L., Thomann, M., Pulfer, M., Lackner, S., 2024. Scattered and transmitted light as surrogates for activated carbon residual in advanced wastewater treatment processes: investigating the influence of particle size. Water Res. X 23.
Li, S., Meng, L., Zhao, C., Gu, Y., Spencer, R.G.M., Álvarez-Salgado, X.A., Kellerman, A. M., McKenna, A.M., Huang, T., Yang, H., Huang, C., 2023. Spatiotemporal response of dissolved organic matter diversity to natural and anthropogenic forces along the whole mainstream of the Yangtze River. Water Res. 234, 119812.
Li, W., Tian, Y., Chen, J., Wang, X., Zhou, Y., Shi, N., 2022. Synergistic effects of sodium hypochlorite disinfection and iron-oxidizing bacteria on early corrosion in cast iron pipes. Front. Environ. Sci. Eng. 16 (6).
Li, W., Zhang, C., Zhang, J., Zhou, Y., Chen, J., Huang, S., 2019. Bio-chemical correlation study on water quality of water supply system under chloramine disinfection. Water Wastewater Eng. 45 (7), 24–31.
Liu, J.C., Ouyang, T., Lu, G.H., Li, M., Li, Y.P., Hou, J., He, C., Gao, P., 2024. Ecosystem risk-based prioritization of micropollutants in wastewater treatment plant effluents across China. Water Res. 263.
Peng, D.H., Zhou, G., An, K., Guo, W.T., Yang, T.T., Kong, W.W., Shen, B.X., Wang, X., Lyu, H., Ma, J., 2025. Critical review on the adsorption of taste and odor compounds by activated carbon: influencing factors, modifications methods, mechanism. Chem. Eng. J. 507.
Perrin, Y., Bouchon, D., Delafont, V., Moulin, L., Hechard, Y., 2019. Microbiome of drinking water: a full-scale spatio-temporal study to monitor water quality in the Paris distribution system. Water Res. 149, 375–385.
Quan, C., Miskolczi, N., Feng, S.X., Grammelis, P., Wu, C.F., Gao, N.B., 2023. Effect of type of activating agent on properties of activated carbon prepared from digested solid waste. J. Environ. Manage. 348.
Ray, S., Roy, K., 2013. Modeling adsorption of organic compounds on activated carbon using ETA indices. Chem. Eng. Sci. 104, 427–438.
Rosenqvist, T., Hilding, J., Suarez, C., Paul, C.J., 2025. Microbial communities in slow sand filters for drinking water treatment adapt to organic matter altered by ozonation. Water Res. 270.
Salama, Y., Chennaoui, M., Sylla, A., Mountadar, M., Rihani, M., Assobhei, O., 2016. Characterization, structure, and function of extracellular polymeric substances (EPS) of microbial biofilm in biological wastewater treatment systems: a review. Desalinat. Water Treat 57 (35), 16220–16237.
Selmi, T., Gentil, S., Fierro, V., Celzard, A., 2024. Enhancing micropollutant removal efficiency using sustainable activated charcoal. J. Environ. Chem. Eng. 12 (6).
Shi, S., Wang, F., Hu, Y., Zhou, J., Zhang, H., He, C., 2024. Effects of running time on biological activated carbon filters: water purification performance and microbial community evolution. Environ. Sci. Pollut. Res. Int. 31 (14), 21509–21523.
Song, W., Li, C., Du, Z., Yue, J., Sun, W., Hou, L., Liu, J., Jia, R., 2021. Research about organic matter removal and biofilms development of pilot-scale UV/H2O2-BAC process. Water 13 (4), 565.
Tao, H., Han, J., Xu, C., 2020. Evaluation of BAC replacement method in drinking water treatment plant. Journal of Huazhong University of Science and Technology. Nature Sci. 48 (8), 121–126.
Teel, L., Pagilla, K., Sundaram, V., Li, L., Guarin, T., Haak, L., 2022. Pathogen reduction by ozone-biological activated carbon-based advanced water reclamation for reuse. Water Environ. Res. 94 (5).
Terry, L.G., Summers, R.S., 2018. Biodegradable organic matter and rapid-rate biofilter performance: a review. Water Res. 128, 234–245.
Vignola, M., Werner, D., Hammes, F., King, L.C., Davenport, R.J., 2018. Flow-cytometric quantification of microbial cells on sand from water biofilters. Water Res. 143, 66–76.
Wan, K., Zhang, M.L., Ye, C.S., Lin, W.F., Guo, L.Z., Chen, S., Yu, X., 2019. Organic carbon: an overlooked factor that determines the antibiotic resistome in drinking water sand filter biofilm. Environ. Int. 125, 117–124.
Wells, M.J.M., Hooper, J., Mullins, G.A., Bell, K.Y., 2022. Development of a fluorescence EEM-PARAFAC model for potable water reuse monitoring: implications for inter-component protein-fulvic- humic interactions. Sci. Total Environ. 820.
Yang, J.S., Yuan, D.X., Weng, T.P., 2010. Pilot study of drinking water treatment with GAC, O3/BAC and membrane processes in Kinmen Island. Taiwan. Desalination 263 (1–3), 271–278.
Zhang, J., Li, W., Chen, J., Wang, F., Qi, W., Li, Y., 2019. Impact of disinfectant on bacterial antibiotic resistance transfer between biofilm and tap water in a simulated distribution network. Environ. Pollut. 246, 131–140.
Zhang, X., Xue, X., Hu, J., 2025. Combined ozonation-biological activated carbon process for antibiotic resistance control in treated effluent from wastewater treatment plant. Water Res. 268.
Zhao, Y.X., Wang, J.Q., Liu, Z.S., Yang, W.L., Hu, J.J., Jia, Z.J., Hu, B.L., 2022. Biofilm: a strategy for the dominance of comammox Nitrospira. J. Clean Prod. 363.
Zhou, Y., Li, W.Y., Qi, W.Q., Chen, S., Tan, Q.W., Wei, Z.Q., Gong, L.C., Chen, J.Y., Zhou, W.Y., 2021. The comprehensive evaluation model and optimization selection of activated carbon in the O_3-BAC treatment process. J. Water Process Eng. 40.